

Deciphering the Regulatory Circuitry That Controls Reversible Lysine Acetylation in *Salmonella enterica*

Kristy L. Hentchel,^a Sandy Thao,^{b*} Peter J. Intile,^{b*} Jorge C. Escalante-Semerena^a

Department of Microbiology, University of Georgia, Athens, Georgia, USA^a; Department of Bacteriology, University of Wisconsin, Madison, Wisconsin, USA^b

* Present address: Sandy Thao, Department of Microbiology, University of Washington, Seattle, Washington, USA; Peter J. Intile, BioTechnology Institute, Department of Microbiology, University of Minnesota-Twin Cities, Saint Paul, Minnesota, USA.

ABSTRACT In *Salmonella enterica*, the reversible lysine acetylation (RLA) system is comprised of the protein acetyltransferase (Pat) and sirtuin deacetylase (CobB). RLA controls the activities of many proteins, including the acetyl coenzyme A (acetyl-CoA) synthetase (Acs), by modulating the degree of Acs acetylation. We report that IolR, a *myo*-inositol catabolism repressor, activates the expression of genes encoding components of the RLA system. *In vitro* evidence shows that the IolR protein directly regulates *pat* expression. An *iolR* mutant strain displayed a growth defect in minimal medium containing 10 mM acetate, a condition under which RLA function is critical to control Acs activity. Increased levels of Pat, CobB, or Acs activity reversed the growth defect, suggesting the Pat/CobB ratio in an *iolR* strain is altered and that such a change affects the level of acetylated, inactive Acs. Results of quantitative reverse transcription-PCR (qRT-PCR) analyses of *pat*, *cobB*, and *acs* expression indicated that expression of the genes alluded to in the IolR-deficient strain was reduced 5-, 3-, and 2.6-fold, respectively, relative to the levels present in the strain carrying the *iolR*⁺ allele. Acs activity in cell-free extracts from an *iolR* mutant strain was reduced ~25% relative to that of the *iolR*⁺ strain. Glucose differentially regulated expression of *pat*, *cobB*, and *acs*. The catabolite repressor protein (Crp) positively regulated expression of *pat* while having no effect on *cobB*.

IMPORTANCE Reversible lysine acylation is used by cells of all domains of life to modulate the function of proteins involved in diverse cellular processes. Work reported herein begins to outline the regulatory circuitry that integrates the expression of genes encoding enzymes that control the activity of a central metabolic enzyme in C2 metabolism. Genetic analyses revealed effects on reversible lysine acylation that greatly impacted the growth behavior of the cell. This work provides the first insights into the complexities of the system responsible for controlling reversible lysine acylation at the transcriptional level in the enteropathogenic bacterium *Salmonella enterica*.

Received 26 May 2015 Accepted 15 June 2015 Published 21 July 2015

Citation Hentchel KL, Thao S, Intile PJ, Escalante-Semerena JC. 2015. Deciphering the regulatory circuitry that controls reversible lysine acetylation in *Salmonella enterica*. mBio 6(4):e00891-15. doi:10.1128/mBio.00891-15.

Editor Stanley Maloy, San Diego State University

Copyright © 2015 Hentchel et al. This is an open-access article distributed under the terms of the [Creative Commons Attribution-Noncommercial-ShareAlike 3.0 Unported license](https://creativecommons.org/licenses/by-nc-sa/4.0/), which permits unrestricted noncommercial use, distribution, and reproduction in any medium, provided the original author and source are credited.

Address correspondence to Jorge C. Escalante-Semerena, jcescala@uga.edu.

This article is a direct contribution from a Fellow of the American Academy of Microbiology.

Reversible lysine acetylation (RLA) is a posttranslational regulatory mechanism present in all domains of life (1). RLA allows an organism to rapidly and reversibly modulate the biological activity of proteins involved in carbon utilization, transcription, translation, and stress responses (2–5) by modulating the acetylation state of the epsilon amino group of lysyl residues critical for function (reviewed in reference 6). In the last decade, studies have provided insights into how the RLA system works in diverse prokaryotes (3, 7–10). As shown in Fig. 1, in *Salmonella enterica*, the RLA system is comprised of a protein acetyltransferase (Pat) of the Gcn5 *N*-acetyltransferase (GNAT) family and an NAD⁺-consuming sirtuin deacetylase (CobB) (2). Relevant to this work is the RLA control of acetyl coenzyme A (acetyl-CoA) synthetase (Acs), an AMP-forming CoA ligase involved in acetate utilization (11). It has been shown that Pat is responsible for the acetylation and inactivation of Acs (2), while removal of the acetyl moiety of AcsAc by the CobB deacetylase

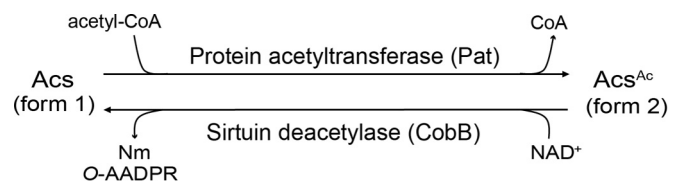


FIG 1 RLA control of acetyl-CoA synthetase (Acs) in *S. enterica*. The activity of the AMP-forming acetyl-CoA synthetase is posttranslationally modified by the protein acetyltransferase Pat. This modification is reversible by the activity of the NAD⁺-consuming class III sirtuin deacetylase CobB. O-AADPR, O-acetyl ADP ribose; Nm, nicotinamide.

reactivates the enzyme (12) (Fig. 1). RLA-dependent regulation of Acs is imperative, as uncontrolled Acs results in growth arrest by depletion of ATP pools (8).

In addition to posttranslational regulation, expression of *acs* is

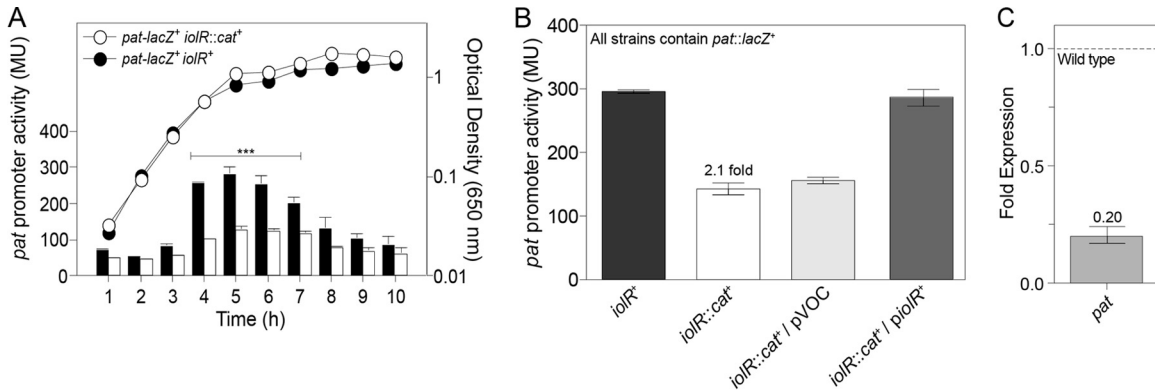


FIG 2 IolR activates *pat* expression *in vivo*. Activity of a *pat-lacZ⁺* chromosomal operon fusion was assessed in the presence (JE7449) or absence (JE10714) of *iolR* to measure *pat* promoter activity (Miller units [MU]) *in vivo* (A and B). Cell cultures were grown at 37°C in NB medium. The data presented are the average of two independent experiments from individual cultures performed in triplicate. Error bars represent standard deviations. The unpaired *t* test gave a *P* value of 0.0004 (A). (C) qRT-PCR showed a 5-fold downregulation in *pat* activity in an *iolR* mutant strain relative to the *iolR⁺* strain. The wild-type transcript level is set at 1, indicated by the dashed line. Error bars represent standard deviations; pVOC, vector-only control.

controlled by several transcriptional regulators (13). While the regulatory region of *cobB* in *S. enterica* has been examined to some extent (14), the transcriptional regulation of genes encoding the enzymes of the RLA system (*pat* and *cobB*) has not been investigated. It has been shown that the catabolite repressor protein (Crp) regulates the *Escherichia coli* *pat* homologue (*pka*) (15), although a role for Crp regulation of *pat* in *S. enterica* has not been reported.

In this work, a genetic approach was used to identify *S. enterica* genes whose products affected the *pat* promoter (P_{pat}). We show that inactivation of *iolR* (*stm4417*), encoding an RpiR-like transcriptional repressor, decreased *pat* expression (16). RpiR-like regulators are involved in sugar catabolism and can function as activators and repressors (17, 18). In *S. enterica*, *Bacillus subtilis*, *Corynebacterium glutamicum*, and *Sinorhizobium meliloti*, IolR negatively regulates expression of the *myo*-inositol utilization operon (16, 19). *myo*-Inositol (cyclohexane-1,2,3,4,5,6-hexol) is an abundant cyclic polyol in soil, and its utilization as a sole carbon source depends on the presence of a large number of genes organized as a genomic island (16), which is present in gamma-proteobacteria, alphaproteobacteria, and some Gram-positive bacteria (20–26).

Here we present *in vivo* evidence that IolR activates *pat* expression in *S. enterica* and that IolR binds to the *pat* promoter *in vitro*. We also report that *acs* and *cobB* are transcriptionally activated by IolR, which places the RLA system of *S. enterica* under IolR control. Significantly, an *iolR* mutant strain displayed a growth defect in minimal medium containing 10 mM acetate, which we suggest is due to an imbalance of the active (nonacetylated)/inactive (acetylated) Acs ratio caused by changes in *pat* and *cobB* expression in the absence of IolR. Finally, we show that Crp, a global regulator of carbon metabolism, regulates *pat* and *acs* expression in *S. enterica*. To our knowledge, this is the first report of global, integrative transcriptional control of genes encoding the enzymes of the RLA system in *S. enterica* and its effect on carbon metabolism.

RESULTS

IolR regulates *pat* expression. A genetic screen was used to identify genes whose functions affected the expression of *pat*, the gene

encoding the protein acetyltransferase in *S. enterica*. Changes in *pat* expression were monitored in strain JE7449, which carried a chromosomal *pat::MudJ* (*lacZ⁺ kan⁺*) reporter (hereafter *pat-lacZ⁺*) (see Table S1 in the supplemental material). This strain was transduced to tetracycline resistance (Tc^r) using a P22 lysate grown on a pool of ~100,000 strains, each of which was assumed to contain one *Tn10d*(*tet⁺*) element randomly inserted in the genome. Tc^r derivatives of the *pat-lacZ⁺* reporter strain (~20,000) were screened for changes in β -galactosidase activity, leading to the identification of two colonies that were less blue than the parental strain. The DNA sequence flanking the *Tn10d*(*tet⁺*) elements located both insertions within *iolR* (*stm4417*), the gene encoding the repressor of the *myo*-inositol utilization (*iol*) genes. No other insertions affecting *pat* expression were identified. To confirm that the *iolR::Tn10d*(*tet⁺*) element was responsible for the reduced expression of the *pat-lacZ⁺* reporter, phage P22 grown on the original *iolR::Tn10d*(*tet⁺*) *pat-lacZ⁺* strain was used to transduce strain JE7449 (*pat-lacZ⁺*) to Tc^r . The reconstructed *iolR::Tn10d*(*tet⁺*) *pat-lacZ⁺* strain (JE10535) displayed the same reduction in *pat-lacZ⁺* expression measured in the original mutant strain (data not shown).

To independently confirm the effect of IolR on *pat* expression, an *iolR::cat⁺* mutation was introduced into strain JE7449 (*pat-lacZ⁺*). Measurements of β -galactosidase activity of the *pat-lacZ⁺* *iolR::cat⁺* strain (JE10714) during growth in nutrient broth (NB) showed a reproducible ~2-fold decrease in *pat* promoter (P_{pat}) activity relative to that in the *pat-lacZ⁺* *iolR⁺* strain (Fig. 2A). Complementation analysis with a wild-type allele of *iolR* provided in *trans* restored *pat* expression to the wild-type level (Fig. 2B). The effect of IolR on *pat* expression was confirmed by quantitative reverse transcription-PCR (qRT-PCR) and showed a 5-fold downregulation of the *pat* transcript in an *iolR::cat⁺* strain compared to the wild type (Fig. 2C). From these data, we concluded that the decrease in *pat* expression in an *iolR* strain was due to the absence of IolR.

The effect of IolR on *pat* expression was tested on acetate (10 mM) and *myo*-inositol (55 mM). In the absence of IolR, *pat-lacZ⁺* expression decreased 1.4-fold on acetate (see Fig. S1A in the supplemental material) and 1.3-fold on *myo*-inositol (Fig. S1B) compared to the levels of expression in the *iolR⁺* strain.

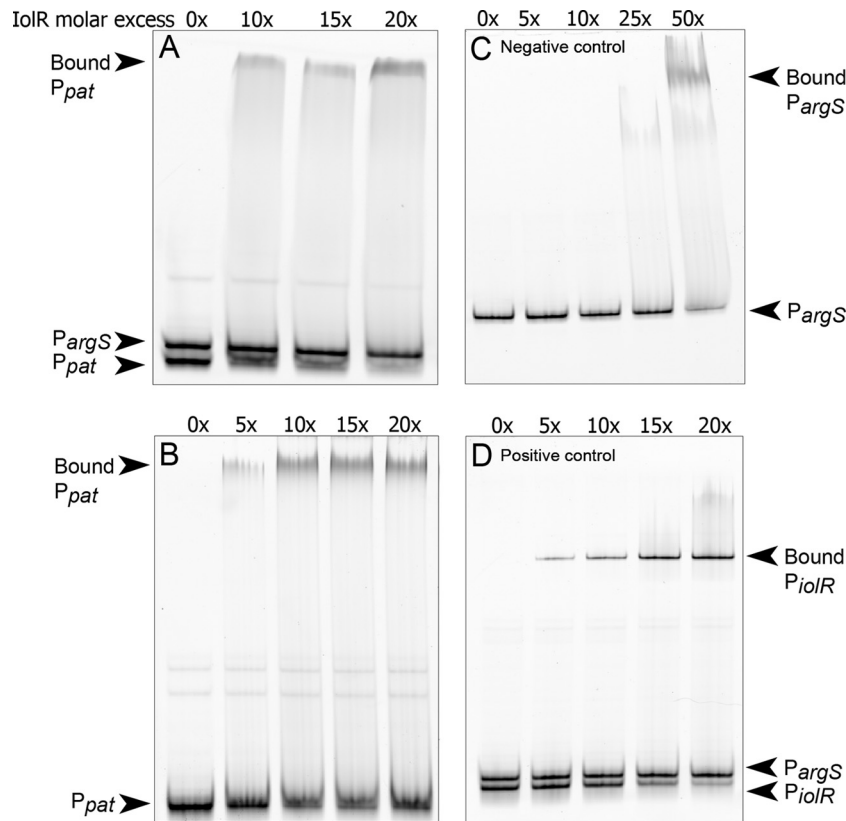


FIG 3 IoLR binds to the *pat* promoter region. Binding of IoLR to the 6-FAM 5'-labeled *pat* promoter (P_{pat} [150 nt, 51 nM]) was analyzed by electrophoretic mobility shift assays in the presence of increasing concentrations of IoLR. (A) P_{pat} and competitor DNA (P_{argS} [196 nt]) were incubated together to show binding specificity of IoLR to P_{pat} . (B) The P_{pat} probe alone was incubated at various concentrations of IoLR. (C) Competitor DNA P_{argS} was incubated with increasing concentrations of IoLR to determine at what point nonspecific binding interactions occur. (D) The interaction between IoLR and P_{iolR} (175 nt) was performed as a known binding control and incubated in the presence of competitor DNA, P_{argS} . The protein concentration shown is in molar excess to the probe (picomoles). EMSAs were performed in triplicate.

Pat does not acetylate IoLR and is not required during growth on myo-inositol. IoLR represses the expression of genes encoding *myo*-inositol-degrading enzymes (16, 27), and it was surprising to find that IoLR may also play a role in the activation of genes comprising the RLA system. We considered the possibility of a regulatory system in which Pat would control the DNA binding activity of IoLR via acetylation, as reported for Pat and the *E. coli* transcription factor RcsB (3). However, we did not obtain any experimental evidence of Pat-dependent regulation of IoLR function under conditions in which acetyl-CoA synthetase (*Acs*), a bona fide Pat substrate (12), was acetylated (see Fig. S2 in the supplemental material).

Consistent with the above-mentioned observation, we determined no difference in the growth rate of the *pat-lacZ*⁺ *iolR::cat*⁺ from that of a strain carrying the wild-type *pat* and *iolR* alleles when grown on *myo*-inositol (see Fig. S3A in the supplemental material). However, the *pat-lacZ*⁺ *iolR*⁺ strain consistently showed a slight but reproducible delay in the onset of growth. As reported by others (16), we observed that the onset of growth of the *iolR::cat*⁺ strain occurred substantially earlier than that of a strain carrying the wild-type *iolR* allele, an observation consistent with the lack of repression of the *myo*-inositol genomic island in a strain devoid of the IoLR repressor (see Fig. S3A).

IoLR is a tetramer. To study the role of IoLR regulation of *pat*, the IoLR protein was isolated to 96% homogeneity (see Fig. S4A in

the supplemental material). The oligomeric state of IoLR was determined using fast protein liquid chromatography (FPLC) gel filtration analysis (see Fig. S4B in the supplemental material). Under the conditions tested, IoLR eluted ~24 min after injection, a retention time consistent with the behavior of a protein whose mass was ~134 kDa compared to elution times of molecular mass standards. Since the predicted molecular mass of IoLR was 31 kDa, it was concluded that IoLR was either a dimer of dimers or a tetramer.

IoLR binds to the *pat* promoter (P_{pat}) *in vitro*. Electrophoretic mobility shift assays (EMSA) were performed to determine if the effect of the IoLR regulator on *pat* expression was the result of direct binding of IoLR to P_{pat} . Experimental promoter analysis data were used to identify the transcription start site (TSS) (<http://www.imib-wuerzburg.de/research/salmonella>) (28). To probe for the specificity of the interaction between IoLR and P_{pat} , we added a nonspecific competitor DNA probe, P_{argS} , previously used to study IoLR binding (16). Increasing concentrations of IoLR shifted the P_{pat} probe but not the P_{argS} probe, a result that supported the conclusion that IoLR directly and specifically interacted with the P_{pat} promoter (Fig. 3A). Increasing amounts of IoLR protein titrated against a fixed amount of the P_{pat} DNA probe without the presence of P_{argS} also yielded increased amounts of IoLR/ P_{pat} complex (Fig. 3B). IoLR did not shift the mobility of P_{argS} until a molar excess of 50× protein was reached, indicative of nonspecific bind-

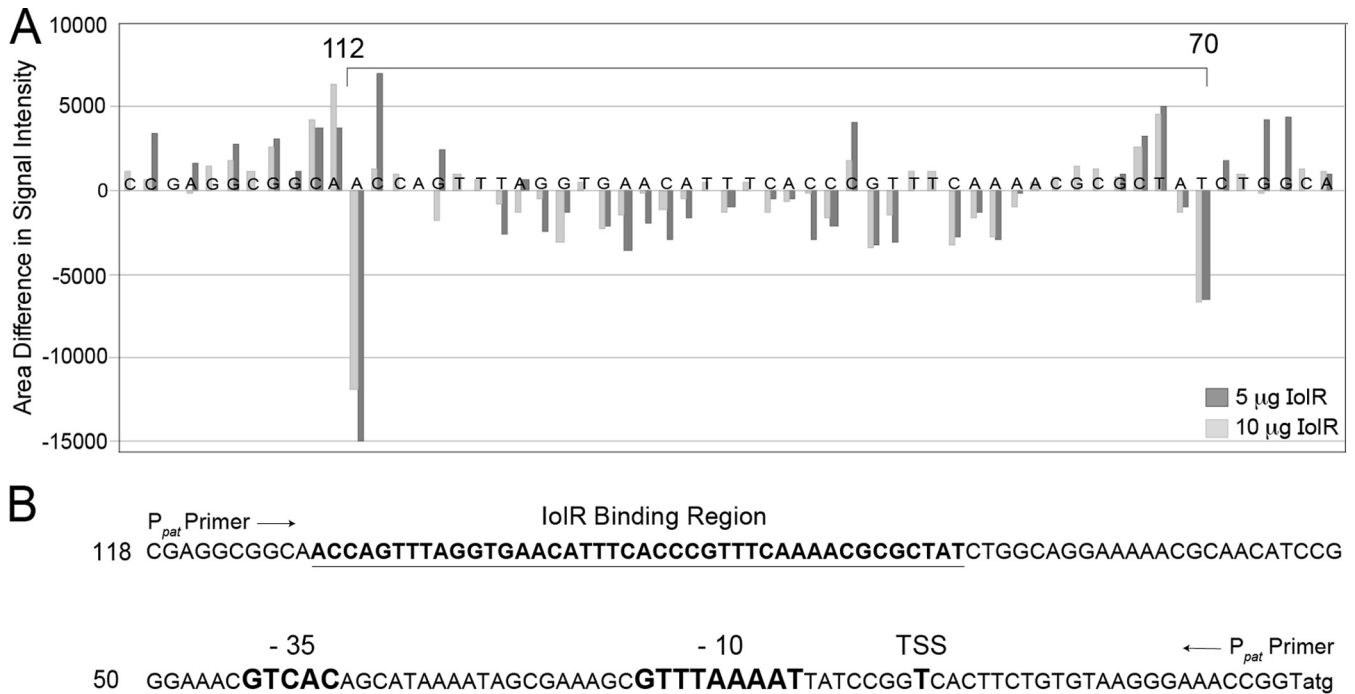


FIG 4 IolR protein binds *pat* promoter at positions -112 to -70 . (A) DNA-footprinting analysis by capillary electrophoresis was used to define the IolR binding region on the *pat* promoter (P_{pat}). On the graph, negative values represent an area of protection, bars indicate the concentration of IolR protein ($5 \mu\text{g}$, dark gray; $10 \mu\text{g}$, light gray), and bar heights represent the area difference between the IolR sample and the negative control (BSA). DNA footprinting was performed and analyzed in two independent experiments. (B) Work by Kröger et al. (28) was used to identify the *pat* transcriptional start site (TSS).

ing of IolR to P_{argS} (Fig. 3C). Previous studies by others showed that IolR negatively regulates the transcription of its own promoter, P_{iolR} (16). Using P_{iolR} (175 nucleotides [nt]) as a positive control with the presence of the competitor probe P_{argS} , we confirmed the reported specificity of IolR for its promoter (16) (Fig. 3D). The P_{pat} and P_{iolR} probes each shifted at similar molar excess concentrations of IolR, supporting the conclusion that IolR directly and specifically interacted with P_{pat} .

Region of the *pat* promoter recognized by IolR. We performed DNA-footprinting analysis to identify the region within the *pat* promoter recognized by IolR. A 6-carboxyfluorescein (6-FAM) 5'-labeled 382-nucleotide probe containing the P_{pat} promoter was incubated with various concentrations of IolR protein or bovine serum albumin (BSA [negative control]). After incubation and subsequent DNase digestion and purification of the DNA, samples were analyzed as described in Materials and Methods. Electropherogram overlays comparing IolR and BSA (negative control) and putative binding sites were analyzed by aligning the sequenced probe data (data not shown). Data presented in Fig. 4 show a region of protection of P_{pat} from nucleotides -112 to -70 relative to the predicted transcription start site (Fig. 4A). Experimental promoter analysis data from Kroger et al. were used to identify the transcription start site (<http://www.imib-wuerzburg.de/research/salmonella>) (28) (Fig. 4B). A region of hypersensitivity was seen at position -112 , an indicator of DNA bending as the result of the binding of a transcriptional regulator, causing an exposed site susceptible to increased cleavage by DNase. A control was performed in which the amount of IolR was doubled in the reaction ($10 \mu\text{g}$). With this increase in protein concentration, we expected an increase in signal intensity, as seen in Fig. 4A.

Previous studies aimed at examining the regulation of the *iol* genomic island in *S. enterica* by IolR repression did not identify a conserved binding site (16, 29). The intent of the DNA-footprinting analysis was to compare the binding region of IolR within P_{pat} to promoter regions regulated by IolR, with the idea of determining a consensus IolR-binding region. While unable to determine a consensus site, the data confirmed the direct interaction between IolR and P_{pat} .

IolR binds to the region of P_{pat} identified by DNA footprinting. A 45-nt probe corresponding to the protected region of P_{pat} identified as the IolR-binding region was used to validate the DNA-footprinting experiments. A 6-FAM 5'-labeled 45-nt probe, P_{pat45} , was generated by annealing complementary primers, and the binding of IolR to this region was examined. The data presented show that IolR binds to the 45-nt probe, confirming that the IolR-binding site is located within this region (see Fig. S5 in the supplemental material). The reason for the presence of signals of higher-molecular-mass complexes is unclear. Possible explanations include the absence of a ligand sensed by IolR or the formation of higher-order IolR multimers. We speculate that this behavior will be better understood as we learn how IolR interacts with P_{pat} .

The absence of IolR impairs growth on 10 mM acetate. Growth of an *iolR::cat⁺* strain was inhibited on 10 mM acetate, with a growth rate three times slower (doubling time of 36 h) (Fig. 5A, solid triangles) than that of a strain carrying the wild-type *iolR* allele (doubling time of 11 h) (Fig. 5A, solid squares). Growth of the *iolR::cat⁺* strain was restored when *iolR* was expressed ectopically (Fig. 5A, open triangles), indicating that the growth defect was due to the absence of IolR. A similar growth defect was reported for an *iolR* mutant strain of *C. glutamicum*, but this obser-

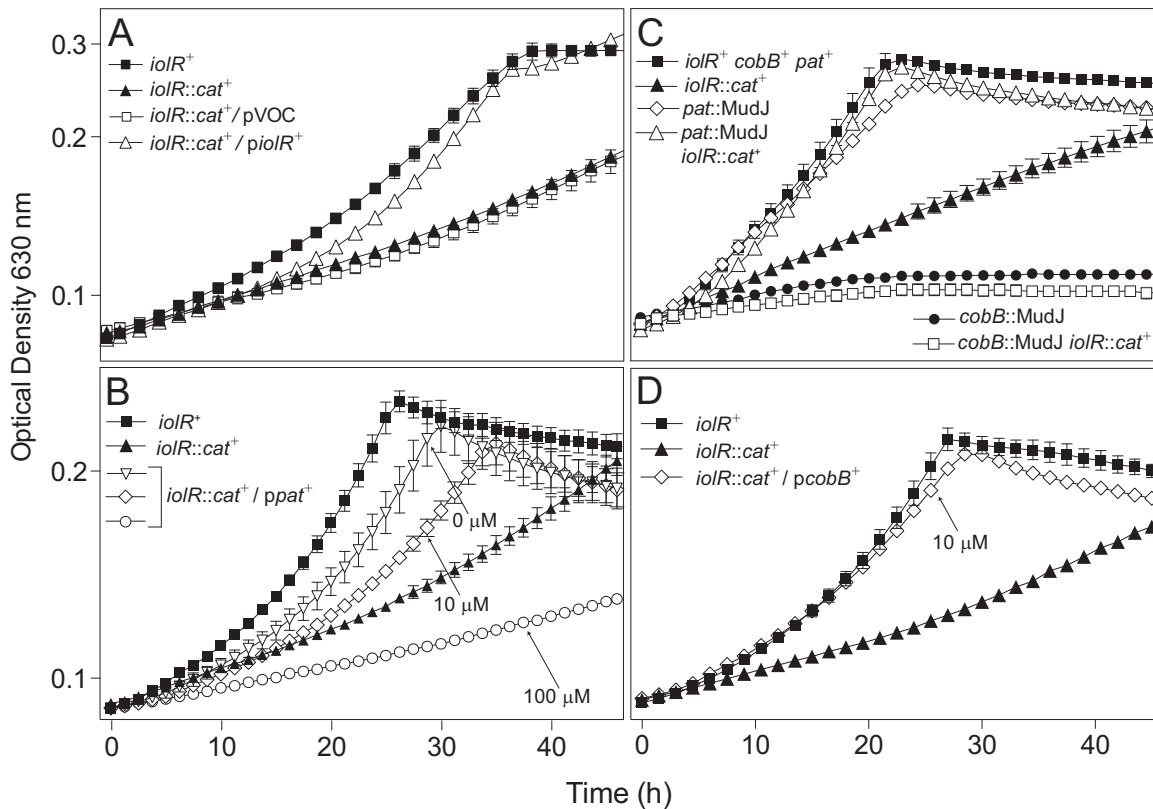


FIG 5 An *iolR* strain has a growth defect on 10 mM acetate. Growth of *S. enterica* strains was examined in NCE minimal medium containing 10 mM acetate. Expression of *iolR* was induced using 100 μM L-(+)-arabinose, *cobB* expression was induced with 10 μM L-(+)-arabinose, and *pat* expression was induced with various concentrations of inducer, as indicated. Growth curves were performed using a Powerwave XS2 microplate reader (Bio-Tek Instruments) at 37°C with shaking in triplicate in three independent experiments. The strains analyzed had the following genotypes: *iolR*⁺ (JE6583), *iolR::cat*⁺ (JE10713), *iolR::cat*⁺/pVOC (JE16934), *iolR::cat*⁺/P_{*iolR*}⁺ (JE16935), *pat*::MudJ (JE7449), *pat*::MudJ *iolR::cat*⁺ (JE10714), *cobB*::MudJ (JE2845), *cobB*::MudJ *iolR::cat*⁺ (JE14972), *iolR::cat*⁺/P_{*pat*}⁺ (JE18927), and *iolR::cat*⁺/P_{*cobB*}⁺ (JE18891). Error bars represent standard deviations. pVOC, vector-only control.

vation was not investigated (27). No growth differences were observed for the *iolR*⁺ *pat*⁺, *iolR::cat*⁺, or *pat*::MudJ strains when grown on 50 mM acetate or glycerol (see Fig. S3C and D in the supplemental material).

Because the observed phenotype on 10 mM acetate correlated with lower levels of *pat* expression, we hypothesized that increases in the expression of *pat* under the control of an IolR-independent promoter would restore growth of the *iolR::cat*⁺ strain on 10 mM acetate. Indeed, the *iolR::cat*⁺ strain grew almost as well as the *iolR*⁺ strain when *pat* was expressed in *trans* (Fig. 5B, inverted triangles). An increase in the level of inducer (10 to 100 μM) compromised growth of the *iolR::cat*⁺/P_{*pat*}⁺ strain. The negative effect of higher *pat* expression was not surprising since increased Pat levels are known to increase the level of acetylated, inactive Acs (8).

The phenotype of the *iolR* strain is caused by an imbalance in the Pat/CobB ratio, which affects Acs activity. In *S. enterica*, Pat and CobB control Acs activity (6). Given that *pat* expression decreased in the *iolR::cat*⁺ strain, we hypothesized that the absence of IolR created an imbalance in the Pat/CobB ratio that favored Pat activity and thus a decrease in Acs activity due to Acs acetylation. We reasoned that such loss of Acs activity could be counteracted in several ways. First, inactivation of *pat* in the *iolR* strain would block Acs acetylation and should restore growth. Indeed, the poor growth of the *iolR* strain on 10 mM acetate (Fig. 5C, solid

triangles) was reversed when *pat* was inactivated (Fig. 5C, open triangles). As expected, a *cobB* strain failed to grow on 10 mM acetate because acetylated Acs could not be reactivated by deacetylation (Fig. 5C, solid circles). Although inactivation of *iolR* presumably reduced Pat levels in the *cobB* strain (by lowering the expression of *pat*), the reduced level was apparently sufficient to keep Acs acetylated (i.e., inactive); thus, growth was not restored (Fig. 5C, open squares). Additionally, inactivation of *pat* in an otherwise wild-type background had minimal effect on growth likely caused by an excess of Acs activity due to CobB deacetylation (2).

Second, if the net result of the change in the Pat/CobB ratio in the *iolR::cat*⁺ strain was an increase in acetylated, inactive Acs, an increase in the level of CobB sirtuin deacetylase in the *iolR::cat*⁺ strain would restore Acs to its active, deacetylated state, and consequently growth on 10-mM acetate would occur. This prediction was confirmed, as shown in Fig. 5D.

Third, if the growth defect of the *iolR::cat*⁺ strain on 10 mM acetate was caused by a change in the level of Acs activity, it followed that overexpression of *acs* in the Δacs *iolR::cat*⁺ strain would restore growth on 10 mM acetate. Results obtained using control strains are shown, and as expected, the Δacs strain failed to grow on 10 mM acetate (Fig. 6A, inverted triangles), and growth was restored by expression of *acs* in *trans* (Fig. 6A, circles). Shown in Fig. 6B is the effect of ectopic synthesis of wild-type Acs in the

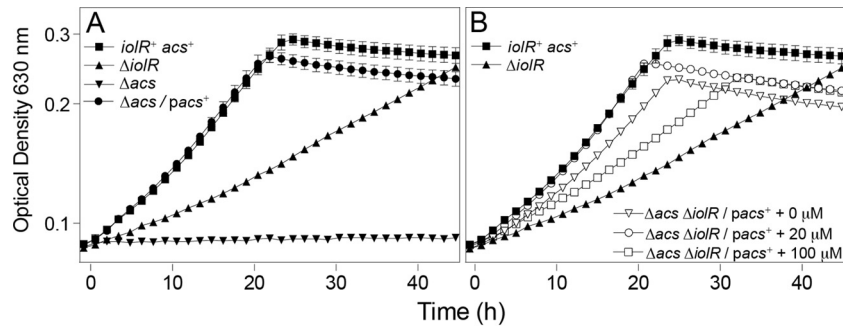


FIG 6 Induction of *acs* expression restores growth of an *iolR* strain on 10 mM acetate. Growth of a *iolR*::*cat*⁺ strain containing *acs* expressed ectopically under the control of an L-(+)-arabinose-inducible promoter was examined in minimal medium containing acetate (10 mM). Control strains are shown in panel A. The effects of *acs* induction are shown in panel B. Growth curves were performed using a Powerwave XS2 microplate reader (Bio-Tek Instruments) at 37°C with shaking in triplicate in three independent experiments. The strains analyzed had the following genotypes: *iolR*⁺ (JE6583), *iolR*::*cat*⁺ (JE10713), Δ *acs* (JE7758), Δ *acs*/*P*_{*acs*}⁺ (JE9912), and Δ *acs* *iolR*::*cat*⁺/*P*_{*acs*}⁺ (JE16596). Expression of *acs* was induced with 0 μ M (open triangles), 20 μ M (open circles), or 100 μ M (black circles in panel A and open squares in panel B). Error bars represent standard deviations.

Δ *acs* *iolR*::*cat*⁺ strain. Wild-type growth of the Δ *acs* *iolR*::*cat*⁺ strain on 10 mM acetate was observed upon induction of *acs* expression [20 μ M L-(+)-arabinose] (Fig. 6B, circles). Unsurprisingly, excessive levels of Acs [100 μ M L-(+)-arabinose] (Fig. 3, open squares) had a deleterious effect on growth, as reported elsewhere (8).

If the growth phenotype of the *iolR*::*cat*⁺ strain on acetate was due to lower Acs activity, we should be able to detect differences in Acs activity in cell-free extracts. Indeed, a reproducible and statistically significant reduction (~25%) in Acs activity was found in cell-free extracts of the *iolR*::*cat*⁺ strain relative to extracts of the *iolR*⁺ strain (Fig. 7).

IolR controls expression of *acs* and *cobB*. Since ectopic expression of *acs* restored growth of the *iolR*::*cat*⁺ mutant, we surmised that *acs* expression was lower in the mutant than in the wild-type strain. To address this possibility we used an *acs-lacZ*⁺ reporter fusion to determine whether IolR was also involved in the regulation of *acs* in *S. enterica*. Since alterations in *pat* expression were likely to affect CobB levels, we also used a *cobB-lacZ*⁺ fusion to assess the effect of the absence of IolR on *cobB* expression. Data obtained from experiments with the above-mentioned transcriptional reporters support the idea that IolR somehow activated expression of both genes (Fig. 8). In the absence of IolR, expression

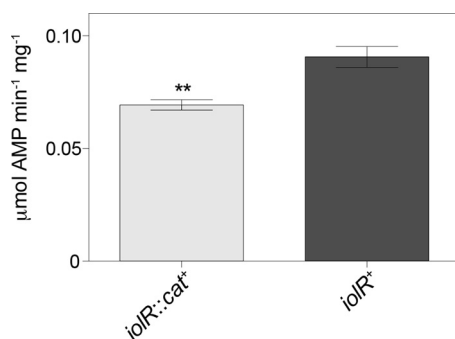


FIG 7 Activity of acetyl-CoA synthetase (Acs). The activity of Acs from whole-cell extracts of an *iolR*⁺ or *iolR*::*cat*⁺ strain grown on acetate (10 mM) was measured using a coupled NADH-consuming spectrophotometric assay (41). The strains analyzed were *iolR*⁺ (JE6583) and *iolR*::*cat*⁺ (JE10713). Samples were analyzed in triplicate. Error bars represent standard deviations. The unpaired *t* test gave a *P* value of 0.002.

of *acs* (Fig. 8A) and *cobB* (Fig. 8B) was reduced on average by 40% (*acs*) or 22% (*cobB*), respectively. The effect of IolR on *acs* and *cobB* expression was confirmed by qRT-PCR and showed a >2-fold and >3-fold downregulation, respectively, of the transcripts in an *iolR*::*cat*⁺ strain compared to the wild type (Fig. 8C). At present, it is unclear whether the effect of IolR on Acs and CobB levels is direct or indirect.

Glucose differentially affects *pat*, *cobB*, and *acs* expression.

Due to the previously established role of the catabolite repressor protein (Crp) in the regulation of the *E. coli* *pat* homologue (*pka*) (15) we examined the effect of catabolite repression on genes encoding the RLA system \pm *iolR*. Expression of *pat* in cells grown in NB plus glucose was reduced by a factor of 2 relative to the expression of *pat* in cells grown in NB lacking glucose (Fig. 9, compare black bars). This suggested that *pat* expression was subjected to catabolite repression, an idea that was further explored. Regardless of the presence of glucose in the medium, the absence of IolR reduced *pat-lacZ*⁺ expression 30 to 40% (Fig. 9A). The absence of IolR had a small but reproducible negative effect (~20%) on *cobB* expression in the absence of glucose, an effect that was magnified to ~40% when glucose was added (Fig. 9B). Significantly, in contrast to *pat* expression, the expression of *cobB* increased ~30% when glucose was added, suggesting that unlike *pat*, expression of *cobB* was not subject to catabolite repression (Fig. 9B, compare black bars).

In *E. coli*, Crp controls the expression of *acs* (30). Consistent with the idea that in *S. enterica* *acs* expression is controlled by catabolite repression, transcription of *acs* was reduced 80% when glucose was present in the medium (Fig. 9C, compare black bars). IolR function also appeared to be important for the activation of *acs* in medium devoid of glucose, with ~50% reduction in *acs* expression in the *iolR*::*cat*⁺ strain relative to the wild type (Fig. 9C, NB medium). In the presence of glucose, expression of *acs* \pm *iolR* was very similar (Fig. 9C, NB plus glucose).

Crp activates *pat* expression. The effect of Crp on *pat* expression was examined in cultures grown in NB plus ribose (10 mM). *P*_{*pat*} activity in the Δ *iolR* *crp*::*cat*⁺ strain was 2.5-fold lower during the mid-log phase than the *P*_{*pat*} activity measured in a strain containing wild-type *iolR* and *crp* alleles (Fig. 10). This decrease in *P*_{*pat*} activity was similar to the one measured in a strain lacking *iolR* and was restored when *crp* was provided in *trans*. *P*_{*pat*} activity was

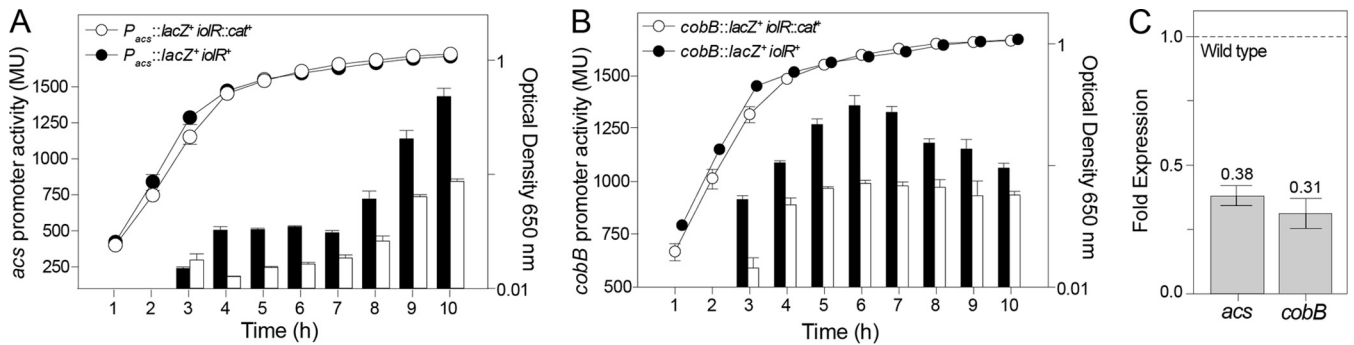


FIG 8 IolR controls expression of *acs* and *cobB*. The activity of *acs-lacZ*⁺ and *cobB-lacZ*⁺ reporters was assessed in backgrounds \pm *iolR* to measure P_{acs} and P_{cobB} activity (Miller units [MU]). Cultures were grown at 37°C in NB medium (A and B). Optical density (650 nm) and β -galactosidase activity (420 nm) were measured hourly. The data were obtained from individual cultures performed in triplicate. Error bars represent standard deviations. The strains analyzed had the following genotypes: *cobB::MudJ* (JE2845), *cobB::MudJ iolR::cat*⁺ (JE14972), $p_{ACS3} P_{acs}$ ⁺ (JE4637), and *iolR::cat*⁺/ $p_{ACS3} P_{acs}$ ⁺ (JE14962). (C) qRT-PCR showed a 2.6-fold downregulation in *acs* activity and a 3-fold decrease in *cobB* activity in an *iolR* strain relative to the *iolR*⁺ strain. The wild-type transcript level is set at 1, indicated by the dashed line. Error bars represent standard deviations.

slightly lower in the $\Delta iolR$ *crp::cat*⁺ strain than that in strains lacking only *crp* or *iolR* (Fig. 10). Collectively, the data indicated that Crp was required for wild-type levels of *pat* expression in *S. enterica*. Pat-dependent acetylation of Crp was tested; however, the data indicate that Pat does not acetylate Crp (see Fig. S2 in the supplemental material).

DISCUSSION

In *S. enterica*, IolR regulates the RLA system. The chief finding from the studies reported herein is that the IolR protein controls and integrates the expression of *pat*, *cobB*, and *acs* (Fig. 2 and 8). Although we do not yet understand the molecular details of how IolR integrates the expression of the above-mentioned genes, collectively our *in vivo* genetic evidence supporting this claim is compelling (Fig. 5 and 6). Furthermore, *in vitro* data obtained support the conclusion that IolR directly interacts with the *pat* promoter (Fig. 3 and 4). Whether or not the effect of IolR on *cobB* and *acs* expression is direct remains to be determined.

IolR function is needed for growth on 10 mM acetate, which requires RLA and Acs. IolR function is necessary for optimal

growth on 10 mM acetate (Fig. 5), and the growth defect of an *iolR* strain suggests that IolR regulation of *pat* and *cobB* impacts the levels of Acs activity in the cell (Fig. 8). This conclusion is supported by data showing that the ectopic expression of *acs* complements growth of an *iolR* strain (Fig. 6). The subtle effects of the absence of IolR on *pat*, *cobB*, and *acs* expression make it difficult to determine the precise magnitude of the changes in Pat, CobB, and Acs protein levels, and in the case of Acs, there is also a need to distinguish between acetylated versus nonacetylated protein. Our attempts to gain insights into these changes using Western blot analysis were unsuccessful due to the lack of required sensitivity to define the magnitude of the predicted changes (data not shown). However, the lower levels of Acs activity present in cell extracts of the *iolR* strain (Fig. 7) support our conclusions.

The differentially responsive effect of glucose on *pat* and *cobB* expression is needed to ensure sufficient activation of acetate by Acs. The differential effect that glucose has on the expression of *pat* and *cobB* (Fig. 9) can be explained by considering the acetogenic nature of glucose. During glucose catabolism, excess acetyl-CoA is diverted through the acetate kinase (AckA)/phosphotrans-

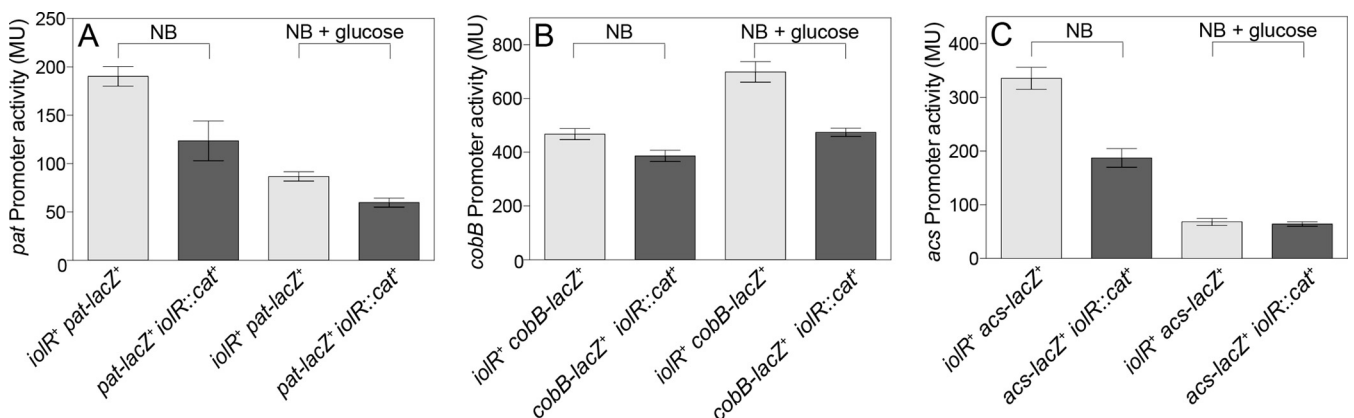


FIG 9 Glucose differentially controls expression of *pat*, *cobB*, and *acs*. Cultures were grown at 37°C in NB medium \pm glucose (10 mM). Optical density (650 nm) and β -galactosidase activity (420 nm) were measured at mid-log phase (OD_{650} of ~ 0.7) to assay for *pat* and *cobB* promoter activity (Miller units [MU]) in a *pat-lacZ*⁺ or *cobB-lacZ*⁺ strain background \pm *iolR*. The data are the average of two independent experiments from individual cultures performed in triplicate. The strains analyzed had the following genotypes: *pat::MudJ* (JE7449), *pat::MudJ iolR::cat*⁺ (JE10714), *cobB::MudJ* (JE2845), *cobB::MudJ iolR::cat*⁺ (JE14972), $p_{ACS3} P_{acs}$ (JE4637), and *iolR::cat*⁺/ $p_{ACS3} P_{acs}$ (JE14962). Error bars represent standard deviations.

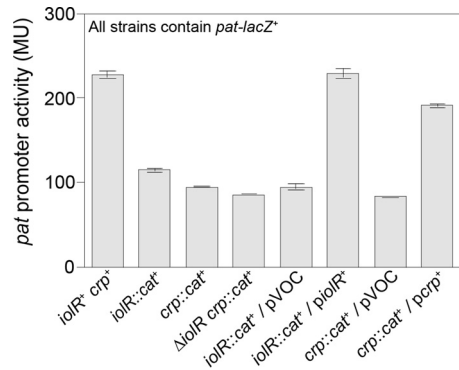


FIG 10 Crp activates *pat* expression. Cultures were grown at 37°C in NB medium with ribose (10 mM). Optical density (650 nm) and β -galactosidase activity (420 nm) were measured at the peak of *pat* expression (OD_{650} of ~0.7) to assay for *pat* promoter activity (Miller units [MU]) in a *pat-lacZ*⁺ strain background. Plasmids were induced with L-(+)-arabinose (100 μ M). The data presented are the average of two independent experiments from individual cultures performed in triplicate. The strains analyzed had the following genotypes: *pat::MudJ* (JE7449), *pat::MudJ iolR::cat*⁺ (JE10714), *pat::MudJ crp::cat*⁺ (JE16743), *pat::MudJ Δ iolR crp::cat*⁺ (JE16744), *pat::MudJ iolR::cat*⁺/pVOC (JE10727), *pat::MudJ iolR::cat*⁺/pIOLR1 (JE10728), *pat::MudJ crp::cat*⁺/pVOC (JE16771), and *pat::MudJ crp::cat*⁺/P_{crp}⁺ (JE17322). Error bars represent standard deviations. pVOC, vector-only control.

acetylase (Pta) pathway, yielding ATP via substrate-level phosphorylation and releasing CoA, which is needed by the pyruvate dehydrogenase to make more acetyl-CoA. In *S. enterica*, the assimilation of glucose-derived acetate is known to require the functions of AckA/Pta and Acs. Notably, during growth on glucose, less Acs is made because Crp cannot fully activate *acs* expression when cyclic AMP (cAMP) levels are low (31). One plausible way the cell can ensure that the limited amount of Acs made by the cell in the presence of glucose supplies enough acetyl-CoA to support growth is to lower the expression of *pat* while increasing the expression of *cobB* (Fig. 9). By so doing, less Acs becomes acetylated, and whatever Acs is acetylated is reactivated by the higher levels of CobB deacetylase made under these conditions. Given that *pat* expression is reduced whenever IolR or Crp is not made, it was surprising to find out that the absence of both regulators did not have an additive effect on *pat* expression (Fig. 10). This result could simply reflect the basal level of *pat* expression or possibly represent a more complex regulatory network in which Crp affects regulation of *iolR*. Such an idea would not be unprecedented, since in *B. subtilis*, the *iol* operon, including *iolR*, is under the control of catabolite repression (32).

Why does IolR activate expression of the RLA system? The dual regulatory role of IolR as a repressor of *iol* genes and an activator of *pat*, *cobB*, and *acs* is intriguing. The ability of IolR to function as an activator is not unprecedented. A report on *C. glutamicum* demonstrated that IolR activates expression of *pck* (encodes phosphoenolpyruvate carboxykinase) (27). IolR also regulates *srff*, coding for a type III secretion effector protein, in *Salmonella* (33), a result that is not surprising as *srff* lies within the *iol* genomic island, which is regulated by IolR.

Under conditions where acetate and *myo*-inositol are simultaneously present in the environment, the cell needs to integrate their metabolism. In thinking about this issue, one must consider that acetate and *myo*-inositol are catabolized at substantially different rates, as acetate enters the central metabolism as soon as it is

converted into acetyl-CoA. In contrast, *myo*-inositol degradation requires the generation of a signal that upon binding to IolR lifts repression of the *iol* genes, and synthesis of *myo*-inositol-degrading enzymes can occur. Generation of the signal needed to transcribe the *iol* genes is apparently an extensive process (see Fig. S3A in the supplemental material for comparison of the differences in lag phases between the *iolR*⁺ and *iolR* strains). The use of IolR to integrate *myo*-inositol and acetate metabolism would be an efficient way to generate as much acetyl-CoA for anabolic purposes as possible while maintaining the capability of modulating the activity of the RLA system for the purpose of controlling the level of Acs activity.

Is *myo*-inositol utilization regulated by RLA? Recently, the total population of acetylated proteins (the “acetylome”) of the *myo*-inositol-utilizing bacteria *B. subtilis* and *Erwinia amylovora* were reported (9, 10). Notably, two enzymes involved in the degradation of *myo*-inositol, malonate semialdehyde dehydrogenase (IolA) and carbohydrate kinase (IolC), were among the acetylated proteins identified. It is unclear whether the activity of IolA and/or IolC is controlled by RLA in either organism or in *S. enterica*. If any Iol proteins are under RLA control, this could provide a link between IolR regulation of RLA and RLA involvement in *myo*-inositol utilization.

MATERIALS AND METHODS

Culture media and chemicals. Nutrient broth (NB) (Difco) containing NaCl (85 mM) was used as rich medium. The minimal medium used was no-carbon essential (NCE) minimal medium (34) containing MgSO₄ (1 mM), Wolfe’s trace minerals (1 \times) (35), and a carbon source (acetate [10 or 50 mM], glycerol [22 mM], or *myo*-inositol [50 mM]). Antibiotics were added at the following concentrations: tetracycline, 20 μ g·ml⁻¹; chloramphenicol, 20 μ g·ml⁻¹; kanamycin, 50 μ g·ml⁻¹; and ampicillin, 100 μ g·ml⁻¹. When added, 5-bromo-4-chloro-3-indolyl- β -D-galactopyranoside (X-Gal) was present at 40 μ g·ml⁻¹, and the calcium chelator ethyleneglycol tetraacetic acid (EGTA) was present at 10 mM. Chemicals were purchased from Sigma-Aldrich.

Bacterial strains. All strains studied were derivatives of *S. enterica* serovar Typhimurium strain LT2 (unless otherwise noted in Table S1 in the supplemental material). All primers used in this study are listed in Table S2 in the supplemental material (IDT, Coralville, IA). Strains carrying a deletion of *iolR* or *crp* were constructed following described protocols (36) (see Text S1 in the supplemental material).

Plasmid construction. Plasmids are listed in Table S1 in the supplemental material. For details on plasmid construction, see Text S1 in the supplemental material.

Isolation of Tn10d(*tet*⁺) insertion in *iolR*. A pool of ~100,000 *S. enterica* strains, each assumed to contain one Tn10d(*tet*⁺) element randomly inserted in the chromosome, was generated as described previously (37). A P22 lysate grown on this pool of strains was used to transduce recipient strain JE7449 (*metE ara pat::MudJ*) to tetracycline resistance (*Tc*^r) on NB agar plates containing X-Gal and EGTA. Colonies displaying altered coloration were freed of phage, and P22 phage lysates were generated to use as donors in crosses with the parental JE7449 strain. The location of the insertion was determined in the reconstructed strains by sequencing the DNA flanking the Tn10d(*tet*⁺) element using a PCR-based protocol with degenerate primers (38). DNA sequencing was performed using BigDye Terminator v3.1 protocols (Applied Biosystems).

Growth studies. Cultures were grown overnight at 37°C in NB and used to inoculate medium with (5% [vol/vol]) in a volume of 200 μ l per well of a 96-well plate. NCE minimal medium containing MgSO₄ (1 mM), Wolfe’s trace minerals (1 \times), and a carbon source (acetate [10 or 50 mM], glycerol [22 mM], or *myo*-inositol [50 mM]) was used. Plasmids were induced with L-(+)-arabinose, as described. Plates were incubated at 37°C

in a Powerwave microplate reader (Bio-Tek Instruments). Data were analyzed using Prism v6 (GraphPad) software.

β -Galactosidase assays. β -Galactosidase activities were determined as described previously (39). Three independent overnight cultures were grown in NB plus ampicillin, subcultured (1:100 [vol/vol]) into 200 ml of medium plus ampicillin, and induced with 100 μ M L-(+)-arabinose. Cultures were grown at 37°C in NB, NB plus ribose (10 mM), NB plus glucose (10 mM), acetate (10 mM), or *myo*-inositol (55 mM) medium. Acetate cultures were inoculated with 2.5% (vol/vol) of overnight culture.

qRT-PCR. Cultures of strains JE10713 (*iolR::cat*⁺) and JE6583 (*iolR*⁺) were grown in NB to an optical density at 600 nm (OD₆₀₀) of 0.6. RNA extraction was performed as described previously (40). cDNA synthesis was performed using iScript cDNA synthesis kit (Bio-Rad). qRT-PCRs were performed using Fast SYBR green master mix (Thermo Fischer) and a 7500 Fast real-time PCR system (Applied Biosystems).

Purification of IoIR and Crp. IoIR was purified to 96% homogeneity by a 2-step nickel affinity chromatography purification using an ÄKTA FPLC system (GE Healthcare). Crp was purified using a 2-step nickel affinity chromatography by gravity column. For protocol details, see Text S1 in the supplemental material.

Analytical gel filtration. Experiments were performed using a Superdex 200 HR 10/30 gel filtration column (GE Healthcare) attached to an ÄKTA FPLC system (GE Healthcare). For protocol details, see Text S1 in the supplemental material.

DNA-binding assays. Electrophoretic mobility shift DNA-binding assays were performed using probes with the fluorophore 6-carboxyfluorescein (6-FAM) attached at the 5' end. Probes were generated by PCR amplification from the *S. enterica* chromosome (for details, see Text S1 in the supplemental material). Probes were purified with the Wizard SV gel and PCR cleanup system (Promega). Reaction mixtures (10 μ l) contained 6-FAM 5'-labeled probe (50 ng), Tris-HCl buffer (50 mM [pH 7.5]), KCl (50 mM), MgCl₂ (10 mM), EDTA (0.5 mM), glycerol (10% [vol/vol]), and IoIR protein (shown in molar excess to probe [2.5 to 10 pmol]). Reaction mixtures were incubated at 22°C for 45 min and resolved on a Criterion 10% native polyacrylamide gel (Bio-Rad) in 0.5 \times Tris-borate-EDTA (TBE) buffer (Tris-HCl [45 mM], boric acid [45 mM], EDTA [1 mM] [pH 8.3]). The signal was detected using a Typhoon Trio⁺ variable mode imager (GE Healthcare) with ImageQuant v5.2 software.

DNA-footprinting analysis. The *pat* promoter (*P*_{*pat*}) was amplified from *S. enterica* genomic DNA using 6-FAM 5'-labeled primer (*P*_{*pat*} 382 FAM) and 3' primer (*P*_{*pat*} 382 Rev). Reaction mixtures contained various amounts of IoIR or bovine serum albumin (BSA [negative control]), Tris-HCl (50 mM [pH 7.5]), KCl (50 mM), MgCl₂ (10 mM), EDTA (0.5 mM), and glycerol (10% [vol/vol]) and were incubated for 10 min at 25°C. The labeled DNA probe (120 ng) was added to the reaction mixture, and the mixture was incubated for 20 min at 25°C, followed by addition of DNase for 5 min at 25°C, and then heat inactivated for 10 min at 78°C. Reaction mixtures were purified using the MinElute PCR purification kit (Qiagen). Samples were analyzed with an Applied Biosystems 3730 DNA analyzer (Plant-Microbe Genomics Facility, Ohio State University) set to the default run module for LIZ600 dye, with 0.1 μ l of size standard (LIZ600), 0.5 to 1.0 μ l of sample, and 9 μ l of HiDi per well. For protocol details, see Text S1 in the supplemental material.

In vitro acetylation assay. Protein acetylation assays were performed as described, using radiolabeled [¹⁴C]acetyl-CoA (2, 7, 14). Briefly, reaction mixtures contained *S. enterica* IoIR (*SeIoIR*) or *SeCrp* (5 μ M) with or without *SePat* (3 μ M). *SeAcs* was used as a positive control. Laboratory stocks of homogeneous *SePat* and *SeAcs* proteins were used in these studies. Reactions were resolved and visualized by SDS-PAGE. Radiolabeled proteins were visualized using a Typhoon Trio⁺ variable mode imager (GE Healthcare) with ImageQuant v5.2 software.

Acetyl-CoA synthetase assay. *Acs* activity was measured from treated whole-cell lysates of *iolR*⁺ (JE6583) and *iolR::cat*⁺ (JE10713) strains using

an NADH-consuming assay as described previously (41). For protocol details see Text S1 in the supplemental material.

SUPPLEMENTAL MATERIAL

Supplemental material for this article may be found at <http://mbio.asm.org/lookup/suppl/doi:10.1128/mBio.00891-15/-/DCSupplemental>.

Text S1, PDF file, 0.2 MB.
Figure S1, PDF file, 0.4 MB.
Figure S2, PDF file, 1.1 MB.
Figure S3, PDF file, 0.5 MB.
Figure S4, PDF file, 0.4 MB.
Figure S5, PDF file, 0.7 MB.
Table S1, PDF file, 0.1 MB.
Table S2, PDF file, 0.1 MB.

ACKNOWLEDGMENTS

This work was supported by PHS grant R01-GM62203 to J.C.E.-S. S.T. was supported by PHS Molecular Biosciences training grant T32-GM07215 and NRSA predoctoral fellowship F31-GM083668.

We thank Chelsey M. VanDrisse, Flavia G. Costa, and Michael Ullmer for technical assistance and Michael Zianni (Plant-Microbe Genomic Facility, Ohio State University) for DNA-footprinting analysis.

REFERENCES

- Smith JS, Brachmann CB, Celic I, Kenna MA, Muhammad S, Starai VJ, Avalos JL, Escalante-Semerena JC, Grubmeyer C, Wolberger C, Boeke JD. 2000. A phylogenetically conserved NAD(+)-dependent protein deacetylase activity in the Sir2 protein family. *Proc Natl Acad Sci U S A* 97:6658–6663. <http://dx.doi.org/10.1073/pnas.97.12.6658>.
- Starai VJ, Escalante-Semerena JC. 2004. Identification of the protein acetyltransferase (Pat) enzyme that acetylates acetyl-CoA synthetase in *Salmonella enterica*. *J Mol Biol* 340:1005–1012. <http://dx.doi.org/10.1016/j.jmb.2004.05.010>.
- Thao S, Chen CS, Zhu H, Escalante-Semerena JC. 2010. N(epsilon)-lysine acetylation of a bacterial transcription factor inhibits its DNA-binding activity. *PLoS One* 5:e15123. <http://dx.doi.org/10.1371/journal.pone.0015123>.
- Hu LI, Chi BK, Kuhn ML, Filippova EV, Walker-Peddakotla AJ, Bäsell K, Becher D, Anderson WF, Antelmann H, Wolfe AJ. 2013. Acetylation of the response regulator RcsB controls transcription from a small RNA promoter. *J Bacteriol* 195:4174–4886. <http://dx.doi.org/10.1128/JB.00383-13>.
- Lima BP, Antelmann H, Gronau K, Chi BK, Becher D, Brinsmade SR, Wolfe AJ. 2011. Involvement of protein acetylation in glucose-induced transcription of a stress-responsive promoter. *Mol Microbiol* 81: 1190–1204. <http://dx.doi.org/10.1111/j.1365-2958.2011.07742.x>.
- Thao S, Escalante-Semerena JC. 2011. Control of protein function by reversible N(epsilon)-lysine acetylation in bacteria. *Curr Opin Microbiol* 14:200–204. <http://dx.doi.org/10.1016/j.mib.2010.12.013>.
- Crosby HA, Heiniger EK, Harwood CS, Escalante-Semerena JC. 2010. Reversible N(epsilon)-lysine acetylation regulates the activity of acyl-CoA synthetases involved in anaerobic benzoate catabolism in *Rhodospseudomonas palustris*. *Mol Microbiol* 76:874–888. <http://dx.doi.org/10.1111/j.1365-2958.2010.07127.x>.
- Chan CH, Garrity J, Crosby HA, Escalante-Semerena JC. 2011. In *Salmonella enterica*, the sirT- dependent protein acylation/deacylation system (SDPADS) maintains energy homeostasis during growth on low concentrations of acetate. *Mol Microbiol* 80:168–183. <http://dx.doi.org/10.1111/j.1365-2958.2011.07566.x>.
- Kim D, Yu BJ, Kim JA, Lee YJ, Choi SG, Kang S, Pan JG. 2013. The acetylproteome of Gram-positive model bacterium *Bacillus subtilis*. *Proteomics* 13:1726–1736. <http://dx.doi.org/10.1002/pmic.201200001>.
- Wu X, Vellaichamy A, Wang D, Zamdborg L, Kelleher NL, Huber SC, Zhao Y. 2013. Differential lysine acetylation profiles of *Erwinia amylovora* strains revealed by proteomics. *J Proteomics* 79:60–71. <http://dx.doi.org/10.1016/j.jprot.2012.12.001>.
- Starai VJ, Escalante-Semerena JC. 2004. Acetyl-coenzyme A synthetase (AMP forming). *Cell Mol Life Sci* 61:2020–2030. <http://dx.doi.org/10.1007/s00018-004-3448-x>.
- Starai VJ, Celic I, Cole RN, Boeke JD, Escalante-Semerena JC. 2002.

- Sir2-dependent activation of acetyl-CoA synthetase by deacetylation of active lysine. *Science* 298:2390–2392. <http://dx.doi.org/10.1126/science.1077650>.
13. Browning DF, Beatty CM, Wolfe AJ, Cole JA, Busby SJ. 2002. Independent regulation of the divergent *Escherichia coli* *nrfA* and *acsP1* promoters by a nucleoprotein assembly at a shared regulatory region. *Mol Microbiol* 43:687–701. <http://dx.doi.org/10.1046/j.1365-2958.2002.02776.x>.
 14. Tucker AC, Escalante-Semerena JC. 2010. Biologically active isoforms of CobB sirtuin deacetylase in *Salmonella enterica* and *Erwinia amylovora*. *J Bacteriol* 192:6200–6208. <http://dx.doi.org/10.1128/JB.00874-10>.
 15. Castaño-Cerezo S, Bernal V, Blanco-Catalá J, Iborra JL, Cánovas M. 2011. cAMP-CRP co-ordinates the expression of the protein acetylation pathway with central metabolism in *Escherichia coli*. *Mol Microbiol* 82:1110–1128. <http://dx.doi.org/10.1111/j.1365-2958.2011.07873.x>.
 16. Kröger C, Fuchs TM. 2009. Characterization of the *myo*-inositol utilization island of *Salmonella enterica* serovar Typhimurium. *J Bacteriol* 191:545–554. <http://dx.doi.org/10.1128/JB.01253-08>.
 17. Sørensen KI, Hove-Jensen B. 1996. Ribose catabolism of *Escherichia coli*: characterization of the *rpiB* gene encoding ribose phosphate isomerase B and of the *rpiR* gene, which is involved in regulation of *rpiB* expression. *J Bacteriol* 178:1003–1011.
 18. Yamamoto H, Serizawa M, Thompson J, Sekiguchi J. 2001. Regulation of the *glv* operon in *Bacillus subtilis*: YfiA (GlvR) is a positive regulator of the operon that is repressed through CcpA and Cre. *J Bacteriol* 183:5110–5121. <http://dx.doi.org/10.1128/JB.183.17.5110-5121.2001>.
 19. Yoshida K, Yamamoto Y, Omae K, Yamamoto M, Fujita Y. 2002. Identification of two *myo*-inositol transporter genes of *Bacillus subtilis*. *J Bacteriol* 184:983–991. <http://dx.doi.org/10.1128/jb.184.4.983-991.2002>.
 20. Sundaram TK. 1972. Regulation of *myo*-inositol catabolism in *Aerobacter aerogenes*. *J Bacteriol* 111:284–286.
 21. Fawole MO. 1976. Inositol dehydrogenase from *Serratia marcescens*. *Z Allg Mikrobiol* 16:327–328. <http://dx.doi.org/10.1002/jobm.3630160412>.
 22. Galbraith MP, Feng SF, Borneman J, Triplett EW, de Bruijn FJ, Rossbach S. 1998. A functional *myo*-inositol catabolism pathway is essential for rhizopine utilization by *Sinorhizobium meliloti*. *Microbiology* 144:2915–2924. <http://dx.doi.org/10.1099/00221287-144-10-2915>.
 23. Fry J, Wood M, Poole PS. 2001. Investigation of *myo*-inositol catabolism in *Rhizobium leguminosarum* bv. *viciae* and its effect on nodulation competitiveness. *Mol Plant Microbe Interact* 14:1016–1025. <http://dx.doi.org/10.1094/MPMI.2001.14.8.1016>.
 24. Kawsar HI, Ohtani K, Okumura K, Hayashi H, Shimizu T. 2004. Organization and transcriptional regulation of *myo*-inositol operon in *Clostridium perfringens*. *FEMS Microbiol Lett* 235:289–295. <http://dx.doi.org/10.1016/j.femsle.2004.04.047>.
 25. Yebra MJ, Zúñiga M, Beauflis S, Pérez-Martínez G, Deutscher J, Monedero V. 2007. Identification of a gene cluster enabling *Lactobacillus casei* BL23 to utilize *myo*-inositol. *Appl Environ Microbiol* 73:3850–3858. <http://dx.doi.org/10.1128/AEM.00243-07>.
 26. Mittal R, Peak-Chew SY, Sade RS, Vallis Y, McMahon HT. 2010. The acetyltransferase activity of the bacterial toxin YopJ of *Yersinia* is activated by eukaryotic host cell inositol hexakisphosphate. *J Biol Chem* 285:19927–19934. <http://dx.doi.org/10.1074/jbc.M110.126581>.
 27. Klaffl S, Brocker M, Kalinowski J, Eikmanns BJ, Bott M. 2013. Complex regulation of the phosphoenolpyruvate carboxykinase gene *pck* and characterization of its GntR-type regulator IolR as a repressor of *myo*-inositol utilization genes in *Corynebacterium glutamicum*. *J Bacteriol* 195:4283–4296. <http://dx.doi.org/10.1128/JB.00265-13>.
 28. Kröger C, Dillon SC, Cameron AD, Papenfort K, Sivasankaran SK, Hokamp K, Chao Y, Sittka A, Hébrard M, Händler K, Colgan A, Leekitcharoenphon P, Langridge GC, Lohan AJ, Loftus B, Lucchini S, Ussery DW, Dorman CJ, Thomson NR, Vogel J. 2012. The transcriptional landscape and small RNAs of *Salmonella enterica* serovar Typhimurium. *Proc Natl Acad Sci U S A* 109:E1277–E1286. <http://dx.doi.org/10.1073/pnas.1201061109>.
 29. Kröger C, Stolz J, Fuchs TM. 2010. *myo*-Inositol transport by *Salmonella enterica* serovar Typhimurium. *Microbiology* 156:128–138. <http://dx.doi.org/10.1099/mic.0.032250-0>.
 30. Browning DF, Beatty CM, Sanstad EA, Gunn KE, Busby SJ, Wolfe AJ. 2004. Modulation of CRP-dependent transcription at the *Escherichia coli* *acsP2* promoter by nucleoprotein complexes: anti-activation by the nucleoid proteins FIS and IHF. *Mol Microbiol* 51:241–254. <http://dx.doi.org/10.1046/j.1365-2958.2003.03824.x>.
 31. Beatty CM, Browning DF, Busby SJ, Wolfe AJ. 2003. Cyclic AMP receptor protein-dependent activation of the *Escherichia coli* *acsP2* promoter by a synergistic class III mechanism. *J Bacteriol* 185:5148–5157. <http://dx.doi.org/10.1128/JB.185.17.5148-5157.2003>.
 32. Yoshida K, Kobayashi K, Miwa Y, Kang CM, Matsunaga M, Yamaguchi H, Tojo S, Yamamoto M, Nishi R, Ogasawara N, Nakayama T, Fujita Y. 2001. Combined transcriptome and proteome analysis as a powerful approach to study genes under glucose repression in *Bacillus subtilis*. *Nucleic Acids Res* 29:683–692. <http://dx.doi.org/10.1093/nar/29.3.683>.
 33. Cordero-Alba M, Bernal-Bayard J, Ramos-Morales F. 2012. SrfJ, a *Salmonella* type III secretion system effector regulated by PhoP, RcsB, and IolR. *J Bacteriol* 194:4226–4236. <http://dx.doi.org/10.1128/JB.00173-12>.
 34. Berkowitz D, Hushon JM, Whitfield HJ, Roth J, Ames BN. 1968. Procedure for identifying nonsense mutations. *J Bacteriol* 96:215–220.
 35. Balch WE, Wolfe RS. 1976. New approach to the cultivation of methanogenic bacteria: 2-mercaptoethanesulfonic acid (HS-CoM)-dependent growth of *Methanobacterium ruminantium* in a pressurized atmosphere. *Appl Environ Microbiol* 32:781–791.
 36. Datsenko KA, Wanner BL. 2000. One-step inactivation of chromosomal genes in *Escherichia coli* K-12 using PCR products. *Proc Natl Acad Sci U S A* 97:6640–6645. <http://dx.doi.org/10.1073/pnas.120163297>.
 37. Kleckner N, Roth J, Botstein D. 1977. Genetic engineering in vivo using translocatable drug-resistance elements. New methods in bacterial genetics. *J Mol Biol* 116:125–159. [http://dx.doi.org/10.1016/0022-2836\(77\)90123-1](http://dx.doi.org/10.1016/0022-2836(77)90123-1).
 38. Caetano-Anollés G. 1993. Amplifying DNA with arbitrary oligonucleotide primers. *PCR Methods Appl* 3:85–94. <http://dx.doi.org/10.1101/gr.3.2.85>.
 39. Miller JH. 1972. Assay of β -galactosidase, p 352–355. In *Experiments in molecular genetics*. Cold Spring Harbor Laboratory, Cold Spring Harbor, NY.
 40. Stead MB, Agrawal A, Bowden KE, Nasir R, Mohanty BK, Meagher RB, Kushner SR. 2012. RNAsnap: a rapid, quantitative and inexpensive, method for isolating total RNA from bacteria. *Nucleic Acids Res* 40:e156. <http://dx.doi.org/10.1093/nar/gks680>.
 41. Garrity J, Gardner JG, Hawse W, Wolberger C, Escalante-Semerena JC. 2007. *N*-Lysine propionylation controls the activity of propionyl-CoA synthetase. *J Biol Chem* 282:30239–30245. <http://dx.doi.org/10.1074/jbc.M704409200>.